Nanoscale

Accepted Manuscript

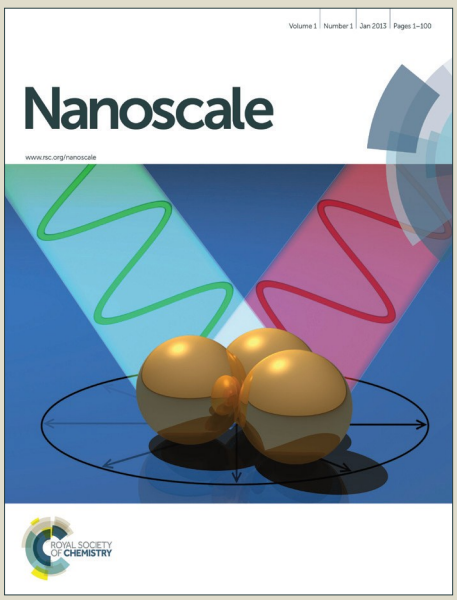

ROYAL SOCIETY OF CHEMISTRY

www.rsc.org/nanoscale

Journal Name

ARTICLE

Large-area high-quality graphene on Ge(001)/Si(001) substrates

I. Pasternak[a], P. Dabrowski[b], P. Ciepielewski[a], V. Kolkovsky[c], Z. Klusek[b], J. M. Baranowski[a], W. Strupinski[a]

Received 00th January 20xx,
Accepted 00th January 20xx

DOI: 10.1039/x0xx00000x

www.rsc.org/

Various experimental data revealing large-area high-quality graphene films grown by the CVD method on Ge(001)/Si(001) substrates are presented. SEM images have shown that the structure of nano-facets is formed on the entire surface of Ge(001), which is covered by a graphene layer over the whole macroscopic sample surface of 1 cm^2. The hill-and-valley structures are positioned 90^0 to each other and run along the <100> direction. The hill height in relation to the valley measured by STM is about 10 nm. Raman measurements have shown that a uniform graphene monolayer covers the nano-facet structures on the Ge(001) surface. Raman spectroscopy has also proved that the grown graphene monolayer is characterized by small strain variations and minimal charge fluctuations. Atomically resolved STM images on the hills of the nanostructures on the Ge(001) surface have confirmed the presence of a graphene monolayer. In addition, the STS/CITS maps show that high-quality graphene has been obtained on such terraces. The subsequent coalescence of graphene domains has led to a relatively well-oriented large-area layer. This is confirmed by LEED measurements, which have indicated that two orientations are preferable in the grown large-area graphene monolayer. The presence of large-area coverage by graphene has been also confirmed by low temperature Hall measurements of a macroscopic sample, showing n-type concentration of 9.3 x 10^{12} cm^{-2} and mobility of 2500 cm^2/Vs. These important characteristic features of graphene indicate a high homogeneity of the layer grown on the large area Ge(001)/Si(001) substrates.

Introduction

During the last ten years graphene as a single layer of carbon with exceptional properties has attracted attention of many scientists and industrialists all over the world. Many papers devoted to graphene characteristics and applications [1-4], graphene synthesis, processing and functionalization have been published [1, 5-7]. So far, graphene for various applications [8-10] has been fabricated by different techniques on diverse substrates and surfaces [1, 7, 11-15]. Up to now researchers have been wondering how to combine graphene's features with its usefulness and appropriate production scale in an optimal manner. Moreover, new promising trends are constantly being observed in graphene research, among which graphene growth on a germanium substrate has generated great interest [16-18]. Such approach to growing graphene on semiconductor surface has been presented as an alternative to graphene growth on the most commonly used copper substrates. While graphene grown on copper substrates has flaws in the form of wrinkles and a boundary between graphene's disoriented flakes [19, 20], graphene obtained on germanium substrates is free from such defects. It is because of the fact that growth of graphene domains and graphene nanoribbons on germanium substrates is self-defining, i.e. these structures reproduce crystal orientation of the substrate and hence when coalescence of the domains occurs they are perfectly matched [17, 21]. Additionally, when focusing on the application of graphene transferred from Cu to stringent high-purity material technology one should be aware of copper contamination associated with the presence of such graphene films, which is typical of transferred layers [22]. Thanks to that approach, one can think about implementing graphene with its extraordinary properties into various fields. Complementary metal oxide semiconductor technology (CMOS) can serve here as a good example of a discipline seriously interested in graphene. One of the developed concepts includes graphene growth on germanium layers deposited directly on Si wafers, used commonly in integrated circuit (IC) manufacturing. This solution guarantees a simple way to apply germanium already compatible with CMOS technology and what is more, one can think about growing graphene directly on the created device structure with predefined active germanium areas. The structure of graphene on Ge(110)/Si(110) wafers has been already described [17]; however, CMOS technology is based on Si wafers with a crystallographic orientation (001), which are commonly and widely used in IC fabrication.

Although graphene growth on germanium wafers has been already presented, there is still a fundamental need to obtain graphene with outstanding physical and electronical properties over a large area. Recently, Kiraly et al. [18] have described both electronic and mechanical features of graphene grown on germanium substrates with three different crystallographic orientations, namely (110), (111) and (001), claiming that graphene is considerably strained in

[a] Institute of Electronic Materials Technology, Wolczynska 133, 01-919 Warsaw, Poland
[b] Department of Solid States Physics, University of Lodz, Pomorska 149/153, Lodz, 90-236, Poland
[c] Institute of Physics Polish Academy of Sciences, AL. Lotnikow 32/46, Warsaw, 02-668 Poland
† Iwona.pasternak@itme.edu.pl

the case of (111) and (110) oriented Ge substrates and extremely strained in the case of (001) oriented Ge substrates. The authors have also observed lower strain values after having annealed the graphene/Ge substrate in vacuum.

In this paper we describe in detail the properties of high-quality graphene grown on Ge(001)/Si(001) wafers. We evaluate the features of graphene films grown over a large area employing complementary techniques. The overriding intention was to present the properties of monolayer graphene on the original substrates, without transferring. Although we synthetize graphene over an area of a few square centimetres, we show graphene features on the maximum reasonable area which can be offered by the used techniques. As an example of the range of researches carried out, we demonstrate the Hall results measured over an area of a 2 x 7 mm Hall bar. In addition, the morphology analyses with the use of scanning electron microscopy (SEM) show a perfectly uniform thickness for a graphene layer across a large area (hundreds of square micrometres). Scanning tunneling microscopy/spectroscopy (STM/STS) study shows a uniform graphene layer with a weak interaction with the substrate grown on reconstructed Ge(001)/Si(001) substrates. X-ray photoelectron spectroscopy results indicated a pure, non-functionalized carbon layer on the surface and a non-oxidized high-quality germanium substrate. What is more, Raman spectroscopy proves the presence of weakly stressed graphene layers on Ge(001)/Si(001) substrates, which is in contradiction to Kiraly's results. Our Raman results were collected on as-grown graphene samples without using additional ex-situ treatment. Moreover, the result of our experiment is high-quality graphene on solid Ge films instead of melted substrates [16]. Through adopting this research methodology we attempted to obtain graphene layers ready to be transferred onto other substrates.

Experimental

Graphene was grown by a CVD method on Ge(001)/Si(001) wafers. The used Ge layers were 3 µm thick films deposited by CVD. During the process of graphene deposition the pressure of 850 mbar was sustained and the temperature was kept constant at 900^0C. Methane gas was used as a carbon precursor in the mixture of Ar in the ratio of 1:200. The step growth was preceded by the substrate's annealing at pure hydrogen atmosphere for in-situ reduction of native oxides [23]. A more detailed description of the growth process is given in our work which has been already accepted for publication [24]. The characterization of the properties of graphene grown directly on Ge(001)/Si(001) substrates was performed at room temperature by Raman spectroscopy using a Renishaw in Via Raman Microscope system with a 532 nm Nd:YAG laser as an excitation source with the laser spot diameter on the sample surface of approximately 0.5 µm. We carried out SEM imaging investigations employing a Hitachi SU8200 Cold Field Emission system. Low energy electron diffraction (LEED) and scanning tunneling microscopy/spectroscopy (STM/STS) including current imaging tunnelling spectroscopy (CITS) were conducted under base pressure of 2×10^{-10} mbar with a Multiprobe P system made by Omicron GmbH (currently Omicron-Scienta). STM/STS measurements were done by the VT-AFM/STM at 110 K and room temperature using a Pt/Ir tip. X-ray, photoelectron spectroscopy (XPS) measurements were performed by the AXIS Supra produced by Kratos under base pressure of 4×10^{-9} mbar using an alumina anode. STM/STS data were visualized by WSXM [25] and the SPIP package.

Results and discussion

The germanium surface itself has been widely investigated in spite of its lower potential for finding technological applications. It was found that Ge(001), Ge(101) and Ge(111) surfaces are planar and belong to the category of major stable surfaces [26]. Despite this, morphological phase transition such as faceting can be observed under certain conditions [27]. Faceting occurs when an initially planar surface is converted to a hill and valley structure. It usually takes place on adsorbate covered single crystal surfaces of many materials [28] and forms a combination of differently oriented steps of nanometer scale dimensions. The step faceting of the Ge(001) surface was observed during heteroepitaxial growth of a strained thin Ge layer on Si(001) [29, 30]. In the context of graphene growth, it was recently revealed that the Ge(001) surface spontaneously breaks up in a hill-and-valley structure in the presence of methane during the graphene growth [21, 31]. Moreover, McElhinny et al. [31] showed that the faceting pattern occurs only in the area where graphene has nucleated and exhibits a four-fold symmetry.

SEM images of graphene grown on Ge(001)/Si(001) were taken from two independent detectors and are shown in Fig. 1. The presented images are representative images taken over a few different diagonal places on the samples. These images revealed different information about the observed sample surface. Fig. 1 a and Fig. 1 b give insights into the composite contrast. One can notice excellent thickness uniformity for the graphene layers. Across the indicated, relatively large area (about 25 x 20 μm^2) only a few minor spots of add-layers of graphene can be recognized. The image is remarkably plain, which indicates a high thickness homogeneity of graphene on the surface of Ge(001). It is also worth emphasizing that there are no wrinkles on the graphene surfaces.

In the case of Fig. 1 c and Fig. 1d, where the topographic contrast is shown, one can observe a characteristic nano-facet pattern on the Ge(001) surface. We have noticed that the nano-facets are formed entirely underneath the graphene layer, which stays in agreement with [31]. Places without graphene, indicated by the lack of Raman signal corresponding to graphene, are also without the nano-facet hill-and-valley pattern. However, in the presented experiments, SEM and Raman spectroscopy allow us to determine the percentage of graphene coverage on the surface of a large macroscopic sample. A typical size of our investigated samples was 1 cm x 1 cm and graphene coverage of the sample in this work was about 100%. The large graphene coverage established by observation of the nano-facet pattern allows us to cut a macroscopic Hall bar and to measure the electrical properties of the grown graphene layer. For magnetotransport measurements of graphene, the graphene/Ge(001)/Si(001) sample in the form of 2 × 7 mm rectangle was equipped with 6 electrical contacts in a Hall bar configuration. Ohmic contacts were formed by indium soldering. The measurements were carried out in the magnetic fields of up to 9 T, applied perpendicular to the plane of graphene at the temperature of 4.2 K to freeze out carriers within the

germanium layer. The concentration of electrons in graphene obtained from the measurement of Hall resistance is $n = 9.3x10^{12}$ cm^{-2} with a mobility of 2500 cm^2/Vs.

A more detailed picture of the nano-facets is shown in STM images presented in Fig. 2. The hill and valley structures are positioned 90^0 to each other, run along the <100> direction and resemble surface faceting that has been observed recently [21]. The hill height in relation to the valley measured by STM is about 10 nm. In order to investigate the morphological features in more detail, graphene grown on Ge(001) samples was carefully studied by STM. Large-scale STM images of graphene covering the Ge(001) surface, which are shown in Fig. 2 a and 2 b, revealed the sample surface with a very high quality. Atomically resolved images of graphene on Ge(001) showed the pristine hexagonal lattice (inset in Fig. 2 b), which indicated the presence of monolayer graphene on terraces of the hill tops of the Ge(001) surface.

Further analysis of graphene quality was performed using the STM/CITS/STS techniques which provide information about the first derivative of the tunneling current in relation to voltage (dI/dV). The dI/dV ratio is proportional to the electron local density of states (LDOS) on the sample surface and such measurements enabled the study of the nanoscale electronic properties of the samples [32]. The STM/CITS/STS results for graphene/Ge(001)/Si(001) are shown in Fig. 3. Nano-scale inhomogeneity in the electronic conductivity of the measured samples is visible on the LDOS map (Fig. 3 b) and correlated with topography presented in Fig. 3 a. The dI/dV spectra shown in Fig. 3 c demonstrate a highly linear characteristic typical for freestanding graphene [33]. This means that graphene layers formed on the hills of Ge(001) nano-facets are not disturbed by interaction with the Ge substrate. In the case of dI/dV measurements conducted between the hills of nano-facets, in the region of valleys, a more quadratic behavior is observed (Fig. 3 d). This may be connected either with a well-known fact that interaction with the substrate can change a linear dispersion relation in graphene [34, 18] or with the presence of a graphene bilayer. However, our Raman spectra (see Fig. 5 a) and atomic resolution STM results suggest that the whole Ge(001) surface is covered by a graphene monolayer. Thus, the existence of the quadratic LDOS behavior in the valley regions seems to be more likely connected with changes in the graphene-substrate interaction than with the presence of a multilayer graphene system. Even though our CITS spectroscopy measurements show a deviation from the linear electron density of states in the valley regions, they demonstrate much better electrical properties for graphene/Ge(001) than has been recently achieved for graphene/Ge(110) and graphene/Ge(111) systems [18]. It is worth noticing that in [18] the linear dependence of LDOS starts to appear at energies higher than the one observed in our experiment. The graphene linear dispersion relation, being disturbed around the Fermi level, indicates that the electrical conductivity cannot be considered in terms of a freestanding model of graphene.

Low-energy electron diffraction (LEED) is used to determine the orientation of the graphene lattice in relation to the underlying Ge(001)/Si(001) substrate. The LEED pattern shown in Fig. 4 a consists mainly of four spots marked with red circles which indicate Ge(001) surface orientation. Furthermore, both intensity and high quality of these spots prove that we are dealing with a clean and perfect germanium layer. It is worth emphasizing that in the case of low-quality substrates, either a blurred pattern or even its lack can be observed. Apart from the Ge(001) pattern, we additionally see superimposed graphene spots along the circles shown in Fig. 4 a as dotted lines. These circles are not centered, i.e. the (00) spots are shifted from one to another. It means that we are dealing with a graphene layer having a number of different orientations in relation to the z-axis coordinate of the LEED spectrometer. Similar results have been recently obtained and discussed by Kiraly et al. [18].

However, a detailed analysis of our LEED data shows some substantial differences. In the previously published paper [18] the LEED pattern consisted of a vast number of blurred spots which constituted easily-distinguishable rings. It means that possible domain orientations along the underlying Ge(001) substrate must be relatively numerous. In our case the spots which constitute each ring can be obtained when we consider two hexagonal cells rotated by 30^0. Therefore, we can conclude that there are only two possible graphene domain orientations along the Ge(001) substrate. The LEED results presented in this work prove that the use of the synthesis method and the choice of the Ge(001)/Si(001) substrate allow growth of a high-quality graphene layer consisting of two domain subsystems.

To investigate the chemical nature of the graphene/Ge interface, X-ray photoelectron spectroscopy (XPS) was used. The C 1s spectrum fitted with a single asymmetric component (Doniach–Sunjic) is shown in Fig. 4 b. The XPS spectrum confirms that carbon present in the system is sp^2 bonded. The Ge 2p peak fitted with a symmetric Voight peak, shown in Fig. 4 c, displays pure chemical characteristics of elemental Ge. The lack of the GeOx peak indicates a minor degree of surface oxidation. Our measurements demonstrate that the Ge(001) surface sustain prolonged exposure to ambient conditions and thermal treatment at 300^0C. In addition, all XPS spectra show also the absence of Ge-C bonds proving graphene integrity.

Raman spectroscopy has been widely used as the tool to characterize various graphene structures [35-39]. In our work we have used confocal Raman spectroscopy, which allows one to use a very small light spot, typically of the order of 0.5 μm [40]. The Raman spectrum presented in Fig. 5a contains two prominent G and 2D peaks and a relatively small, disorder-related D peak near 1350 cm^{-1}. The observed symmetric Lorentzian line shape of the 2D peak is a feature confirming the presence of predominantly single layer graphene. It is known that both Raman G and 2D peaks are sensitive to charge fluctuations and to strain due to the difference in the thermal expansion coefficients of graphene and the underlying substrate. The G peak is mainly dependent on charges present on graphene due to the static effects on the bond lengths and non-adiabatic electron phonon coupling [41]. The 2D peak is predominantly dependent on strain fluctuations and varies in our sample from 2695 cm^{-1} to 2704 cm^{-1}. The Raman map of the position of the 2D peak in the area of 10 x 10 μm^2 taken with a step of 0.5 μm is shown in Fig. 6 a. It is seen that a characteristic pattern of the Ge(001) surface is not reflected in strain distribution shown in Fig. 6. This is due to a large light spot in confocal Raman measurements (about 0.5 μm) and the hill and valley structures present on the Ge(001) surface. For these two reasons, the microscopic properties of graphene on the nanometer scale cannot

be revealed. Therefore, the distribution of strain across the sample shown in Fig. 6 a seems to be random. The same conclusion can be drawn from the Raman map of the position of the G line in the same area of 10 x 10 μm^2 shown in Fig. 6 b. The charge fluctuations reflected in the position of the G peak within the range from 1588 cm^{-1} to 1593 cm^{-1} do not reflect nanometer-scale microscopy of the Ge(001) surface as well.

The line width of the 2D (FWHM) peak usually is considered as a measure of number of layers [33, 37, 42]. However, as it was recently shown that FWHM of the 2D peak is also highly sensitive to strain inhomogeneity in the length of nanometer scales [40, 43]. The average value of the FWHM of the 2D peak shown by histogram in Fig 5 b is about 37 cm^{-1}. This FWHM is much higher than the observed for graphene monolayer on hBN [40]. However, it may correspond for epitaxial graphene monolayer due to microscopic strain variations in length scales bellow the laser spot size. The average spatial distribution of strain and charge doping in the graphene layer can be determined and separated from each other. The contribution from strain and charge doping can be de-convoluted using vector decomposition within the position of the 2D peak E(2D) vs positions of the G peak E(G) space [44]. Plotting of the position of the 2D peak versus the position of the G peak, taken over 20 x 10 μm^2 area shown in Fig.7 a, reveals a variation of compressive strain and doping of graphene in the sample. The spatial spread of the 2D peak position is from 2694 cm^{-1} to 2704 cm^{-1}, and in the G peak position it ranges from 1587 cm^{-1} to 1593 cm^{-1}. The scatter of data points lies at line with a slope of 2.2. This slope coincides with the ratio of strain-induced shifts reported previously [45]. The analysis of the E(2D) vs E(G) diagram may be done in the same way as was done previously [18, 44]. An average strain sensitivity factor of 69.1 cm^{-1}/% can be used [45, 46]. Assuming the strain to be biaxial nature the spread of data indicate variation of compressive strain between -0.37%<ε<-0.25%. The origin of the circled point in Fig. 7 a corresponds to suspended freestanding monolayer graphene (position of the G band 1580 cm^{-1} [47] and the 2D band 2679 cm^{-1} [48]) which is known to be charge neutral. Such strain variation are characteristic for several other our samples. It is interesting that the measured by us Raman spectra show a relatively small average strain variation, significantly smaller than the observed previously on graphene grown on Ge(001) [18]. This is most likely due to uniform faceting of the Ge(001) surface on a relatively large area of the sample.

Finally, the histogram of the intensity ratio of the 2D peak to the G peak (I(2D)/I(G)) shown in Fig. 7 b with the average value close to 2.4 indicates predominantly a monolayer graphene layer structure. This suggests that a relatively high value of FWHM of the 2D peak may be mainly due to nanometer-scale strain variations in graphene on the patterned Ge(001) surface.

Conclusions

All experimental results presented in this work indicate that uniform wrinkle-free graphene layers have been grown on macroscopic Ge(001)/Si(001) substrates. The observation of the nano-facet pattern underneath the graphene layer and Hall measurements proved that the uniform graphene layer has been obtained on the large size samples measuring 1 cm x 1 cm. The uniformity of the predominantly graphene monolayer has been also confirmed by SEM and Raman measurements.

The mechanism responsible for uniform growth lies in the well-ordered nano-facet formation observed in the case of the Ge(001) surface. Apparently, graphene nucleation reproduces the Ge(001) nano-faceting. Most likely, growth originates on the terraces of the hill structures which are well-oriented in the <100> direction. Atomically resolved images of graphene on the terraces of the Ge(001) surface have revealed the presence of a monolayer. In addition, the STS/CITS maps show that high-quality graphene has been obtained on such terraces. The subsequent coalescence of graphene domains leads to a relatively well-oriented large-area layer. However, due to the perpendicular orientation of the terraces merging in the case of graphene domains, the entire layer is not monocrystalline. This is confirmed by LEED measurements, which indicate that in spite of the polycrystalline character of the layer, two orientations within the graphene layer are preferable.

Acknowledgements

The research leading to these results has received funding from the European Union Seventh Framework Programme under grant agreement n°604391 Graphene Flagship. This work was also financially supported by the Polish National Centre within the framework of the DEC-2012/05/B/ST5/00354 Project.

References

1 K. S. Novoselov, A. K. Geim, S. V. Morozov, D. Jiang, Y. Zhang, S. V. Dubonos, I. V. Grigorieva, A. A. Firsov Electric Field Effect in Atomically Thin Carbon Films Science, 2004, **306**, 666–669

2 Daniel R. Cooper, Benjamin D'Anjou, Nageswara Ghattamaneni, Benjamin Harack, Michael Hilke, Alexandre Experimental review of graphene ISRN Condensed Matter Physics Vol. 2012, Article ID 501686

3 A. K. Geim, K. S Novoselov,. The rise of graphene, Nat. Mater., 2007 **6**, 183–197

4 A. K. Geim, Graphene: Status and Prospects, Science, 2009 **324**, 1530–1534

5 Y. Hernandez, et al., High-yield production of graphene by liquid-phase exfoliation of graphite Nature Nanotech 2008 **3**, 563

6 C. Berger, Z Song, X. Li, X. Wu, N. Brown, C. Naud, D. Mayou, T. Li, J. Hass, A. N. Marchenkov, E. H. Conrad, P. N. First, W. A. de Heer, Electronic confinement and coherence in patterned epitaxial graphene Science 2006, **312**, 1191–1195;

7 W. Strupinski, K. Grodecki, A. Wysmolek, R. Stepniewski, T. Szkopek, P. E. Gaskell, A. Gr€uneis, D. Haberer, R. Bozek, J. Krupka, J. M. Baranowski Graphene Epitaxy by Chemical Vapor Deposition on SiC NanoLett. 2011, **11**, 1786–1791

8 Z. Chen, Y.-M. Lin, M. J. Rooks, and P. Avouris, "Graphene nano-ribbon electronics," Physica E: Low-dimensional Systems and Nanostructures, 2007, **40**, 228–232,

9 V. M. Karpan, G. Giovanneti, P. A. Khomyakov, M. Talanana, A. A. Starikov, M. Zwierzycki, J. van den Brink, G. Brocks, and P. J. Kelly, Graphene and graphite as perfect spin filters, Phys. Rev. Lett., 2007, **99,** 176602

10 G. Sobon, J. Sotor, I. Pasternak, A. Krajewska, W. Strupinski, K. M. Abramski All-polarization maintaining, graphene-based

femtosecond Tm-doped all-fiber laser Optics Express 2015 **23**, 9339-9346
11 S. Stankovich, D. A. Dikin, G. H. B. Dommett, K. M. Kohlhaas, E. J. Zimney, E. A. Stach, R. D. Piner, S. T. Nguyen, R. S. Ruoff, Graphene-based composite materials Nature, 2006, **442**, 282
12 W. A. de Heer, C. Berger, X. Wu, P. N. First, E. H. Conrad, X. Li, T. Li, M. Sprinkle, J. Hass, M. L. Sadowski, M. Potemski, G. Martinez, Epitaxial graphene Solid State Commun., 2007, **143**, 92
13 Eizenberg, J. M. Blakely, Carbon Monolayer Phase Condensation on Ni (111), Surf. Sci., 82, 228 1979
14 A. Reina, X. Jia, J. Ho, D. Nezich, H. Son, V. Bulovic, M. S. Dresselhaus, and J. Kong, Large area, few-layer graphene films on arbitrary substrates by chemical vapor deposition Nano Lett. 2009, **9**, 30
15 J. C. Hamilton, J. M. Blakely, Carbon segregation to single-crystal surfaces of Pt, Pd, and Co, Surf. Sci., 91, 199 1980;
16 G. Lippert, J. Dąbrowski, T. Schroeder, M. A. Schubert, Y. Yamamoto, F. Herziger, et al. Graphene grown on Ge(001) from atomic source Carbon 2014, **75**, 104-112
17 Jae-Hyun Lee, Eun Kyung Lee, Won-Jae Joo, Yamujin Jang, Byung-Sung Kim, Jae Young Lim, et al. Wafer-Scale Growth of Single-Crystal Monolayer Graphene on Reusable Hydrogen-Terminated Germanium Science 2014, **344**, 286-289
18 Kiraly B., Jacobberger RM., Mannix AJ, Campbell GP, Bedzyk MJ, Arnold MS, Hersam MC, Guisinger NP., Electronic and Mechanical Properties of Graphene-Germanium Interfaces Grown by Chemical Vapor Deposition Nano Lett. 2015 **15** 7414-20
19 Li, X.; Cai, W.; An, J.; Kim, S.; Nah, J.; Yang, D.; et al. Large-Area Synthesis of High-Quality and Uniform Graphene Films on Copper Foils Science 2009, **324**, 1312–1314
20 Pinshane Y. Huang, Carlos S. Ruiz-Vargas, Arend M. van der Zande, William S. Whitney, Mark P. Levendorf, Joshua W. Kevek, Shivank Garg, Jonathan S. Alden, Caleb J. Hustedt, Ye Zhu, Jiwoong Park, Paul L. McEuen & David A. Muller Grains and grain boundaries in single-layer graphene atomic patchwork quilts Nature 2011, **469**, 389–392
21 Jacobberger, R. M. Et al. Direct oriented growth of armchair graphene nanoribbons on germanium. Nat. Commun. 6 :8006 doi : 10.1038/ncomms9006 (2015)
22 Lupina, G., Kitzmann, J., Costina, I., Lukosius, M., Wenger, C., Wolff, A., et al. Residual metallic contamination of transferred chemical vapor deposited graphene ACS Nano 2015, **9**, 4776–4785
23 Ryosuke Hasegawa, Toshio Kurosawa, and Tetsuo Yagihashi Hydrogen Reduction of Germanium Dioxide, Transactions of the Japan Institute of Metals, 1972, **13**, 39-44
24 I. Pasternak, M. Wesolowski, I. Jozwik, M. Lukosius, G. Lupina, P. Dabrowski, J.M. Baranowski, W. Strupinski, Graphene growth on Ge(100)/Si(100) substrates by CVD method Scientific Reports 2016 DOI:10.1038/srep21773
25 I. Horcas, R. Fernández, J.M. Gómez-Rodríguez, J. Colchero, J. Gómez-Herrero, a M. Baro, WSXM: a software for scanning probe microscopy and a tool for nanotechnology., Rev. Sci. Instrum. 2007, **78** 013705
26 Zheng Gai, W.S. Yang, R.G. Zhao, and T. Sakurai, Macroscopic nanoscale faceting of germanium surfaces Phys. Rev. B, 1999, **59** 15230
27 H.J.W. Zandvliet, O. Gurlu, R. van Gastel, and Bene Poelsema, Faceting of <010> steps on Si(001) and Ge(001) surfaces, Phys. Rev. B 2004, **69**, 125311
28 Theodore E. Madey, Wenhua Chen, Hao Wang, Payam Kaghazchi and Timo Jacob, Nanoscale surface chemistry over faced substrates: structure, reactivity and nanotemplates, Chem. Soc. Rev. 2008, **37**, 2310
29 Y.-W. Mo, D.E. Savage, B.S. Swartzentruber and M.G.Lagally, Kinetic Pathway in Stranski-Krastanov Growth of Ge on Si(001), Phys. Rev. Lett. 1990, **65**, 1020
30 G.-H. Lu and F. Liu, Towards Quantitative Understanding of Formation and Stability of Ge Hut Islands on Si(001) Phys. Rev. Lett. 2005, **94**, 176103
31 Kyle M. McElhinny, Robert M. Jacobberger, Alexander J. Zaug, Michel S. Arnold, and Paul G. Evans, Graphene-induced Ge(001) surface faceting, Surface Science 2016, dx.doi.org/10.1016/j.susc.2015.12.035
32 J. Tersoff, D.R. Hamann, Theory and application for the scanning tunneling microscope, Phys. Rev. Lett. 1983, **50** 1998–2001.
33 J. Xue, J. Sanchez-Yamagishi, D. Bulmash, P. Jacquod, A. Deshpande, K. Watanabe, et al., Scanning tunnelling microscopy and spectroscopy of ultra-flat graphene on hexagonal boron nitride, Nat Mater. 2011, **10** 282–285
34 P. A. Khomyakov, G. Giovannetti, P. C. Rusu, G. Brocks, J. van den Brink, and P. J. Kelly First-principles study of the interaction and charge transfer between graphene and metals, Phys. Rev. B 2009, **79**, 195425
35 A.C. Ferrari, J.C. Meyer, V. Scardaci, C. Casiraghi, M. Lazzeri, F. Mauri, S. Piscanec, D. Jiang, K.S. Novoselov, S. Roth, A.K. Geim, Raman spectrum of graphene and graphene layers, Phys. Rev. Lett., 2006, **97**, 187401
36 T. Mohiuddin, A. Lombardo, R. Nair, A. Bonetti, G. Savini, R. Jalil, N. Bonini, D. Basko, C. Galiotis, N. Marzari, K. Novoselov, A. Geim, A.C. Ferrari, Uniaxial strain in graphene by Raman spectroscopy: G peak splitting, Grüneisen parameters, and sample orientation, Phys. Rev. B, 2009, 79 205433
37 L.O. Nyakiti, R.L. Myers-Ward, V.D. Wheeler, E.A. Imhoff, F.J. Bezares, H. Chun, J.D. Caldwell, A.L. Friedman, B.R. Matis, J.W. Baldwin, P.M. Campbell, J.C. Culbertson, C.R. Eddy, G.G. Jernigan, D.K. Gaskill, Bilayer graphene grown on 4H-SiC(0001) step-free mesas Nano Lett., 2012, **12** 1749–1756
38 J. Röhrl, M. Hundhausen, K.V. Emtsev, T. Seyller, R. Graupner, L. Ley, Raman spectra of epitaxial graphene on SiC(0001), Appl. Phys. Lett., 2008, 92, 201918
39 J. Yan, Y. Zhang, P. Kim, A. Pinczuk, Electric field effect tuning of electron–phonon coupling in graphene, Phys. Rev. Lett., 2007, 1 1–4
40 C.Neumann, S.Teichardd, P.Venezuala, M.Drogeler, L.Banszerus, M.Schmitz, K.Watanabe, T.Taniguchi, F.Mauri, B.Beschoten, S.V.Rotkin and C.Stampfer, Raman spectroscopy as probe of nanometer-scale strain variations in graphene, Nature Comm. 2015, **6**, Article number: 8429
41 M.Lazzeri and F.Mauri, Nonadiabatic Kohn Anomaly in a Doped Graphene Monolayer Phys. Rev.Lett. 2006, **97**, 266407
42 L.M. Malard, M.A. Pimenta, G. Dresselhaus, M.S. Dresselhaus, Raman spectroscopy in graphene, Phys. Rep., 2009, 473, 51–87
43 N.J.G.Couto, D.Costanzo, S.Engels, Dong-Ken Ki, K.Watanabe, T.Taniguchi, C.Stampfer, F.Guinea and A.Morpurgo, Random Stain Fluctuations as Dominant Source for High-Quality On-Substrate Graphene Devices, Phys. Rev. X, 2014, **4**, 041019
44 Ji Eun Lee, Gwanghyun Ahn, Jishim, Young Sik Lee and Sunmin Ryu, Optical separation of mechanical strain from charge doping in graphene Nature Comm. 2012, **3**, 1024
45 T.M.G. Mohiuddin A. Lombardo, R. R. Nair, A. Bonetti, G. Savini, R. Jalil, N. Bonini, D. M. Basko, C. Galiotis, N. Marzari, K. S. Novoselov, A. K. Geim, and A. C. Ferrari, Uniaxial strain in graphene by Raman spectroscopy: G peak splitting, Grüneisen parameters, and sample orientation Phys. Rev. B 2009, **79**, 205433
46 J.Zabel, R. Nair, A. Ott, T. Georgiou, A. K. Geim, K. S. Novoselov, C. Casiragh, Raman Spectroscopy of Graphene

and Bilayer under Biaxial Strain:Bubbles and Balloons Nano Lett. 2012, **12**, 617

47 Stéphane Berciaud, Sunmin Ryu, Louis E. Brus and Tony F. Heinz, Probing the Intrinsic Properties of Exfoliated Graphene: Raman Spectroscopy of Free-Standing Monolayers, Nano Lett., 2009, **9**, 346–352

48 K. Grodecki, J. A. Blaszczyk, W. Strupinski, A. Wysmolek, R. Stepniewski, A. Drabinska, M. Sochacki, A. Dominiak, and J. M. Baranowski, Pinned and unpinned epitaxial graphene layers on SiC studied by Raman spectroscopy, J. Appl. Phys. 2012, **111**, 114307

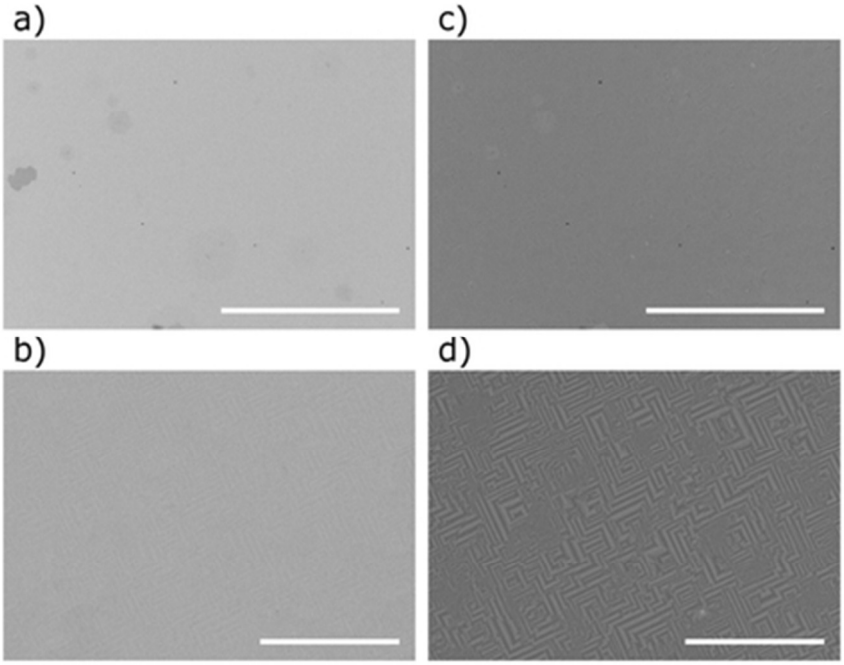

Fig. 1 SEM images of a, b) material contrast and c, d) topography features of graphene grown on Ge(001)/Si(001) wafers. Scale bars are 10 μm for images (a) and (c) and 2 μm for (b) and (d).
38x28mm (300 x 300 DPI)

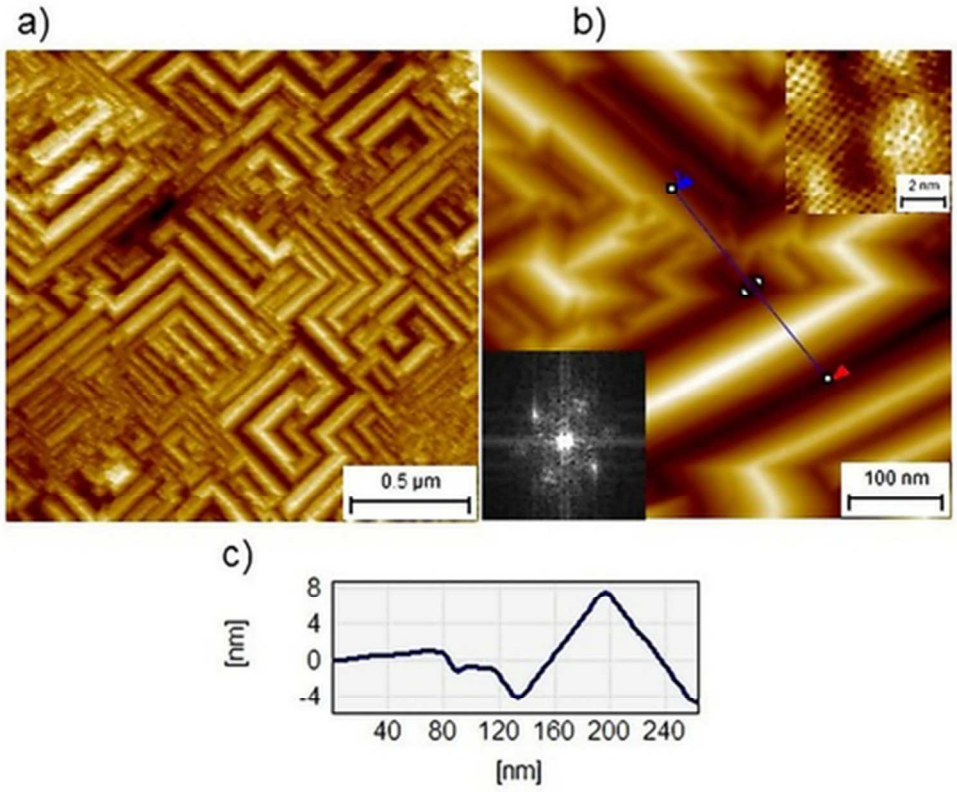

Fig. 2 Scanning tunnelling microscopy images of graphene on Ge(001)/Si(001): a) large-area topography (I= 100 pA, U=0.3 V), b) close look at high-quality graphene/Ge(001)/Si(001) substrate showed reconstruction characteristic of the Ge(001) surface. The top inset reveals an atomically resolved graphene lattice on Ge(001)/Si(001) (I= 300 pA, U=0.1 V). The bottom inset: Fourier transform (FT) showing a hexagonal symmetry of graphene, c) cross section along the blue line in Fig. 2 b.
41x34mm (300 x 300 DPI)

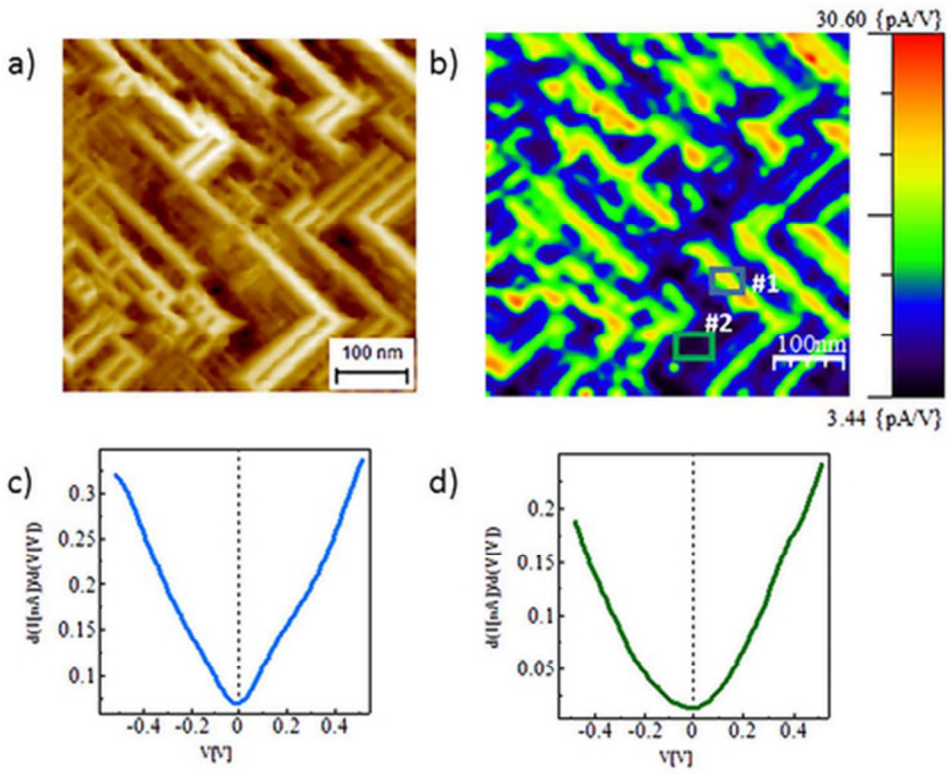

Fig. 3 STM/CITS/STS results obtained for graphene on the Ge(001)/Si(001) substrate. a) STM topography, b) LDOS map measured close to the Fermi level and correlated with topography shown in a). The c) and d) STS curves showing the dI/dV dependences measured in #1 and #2 areas, respectively.
40x32mm (300 x 300 DPI)

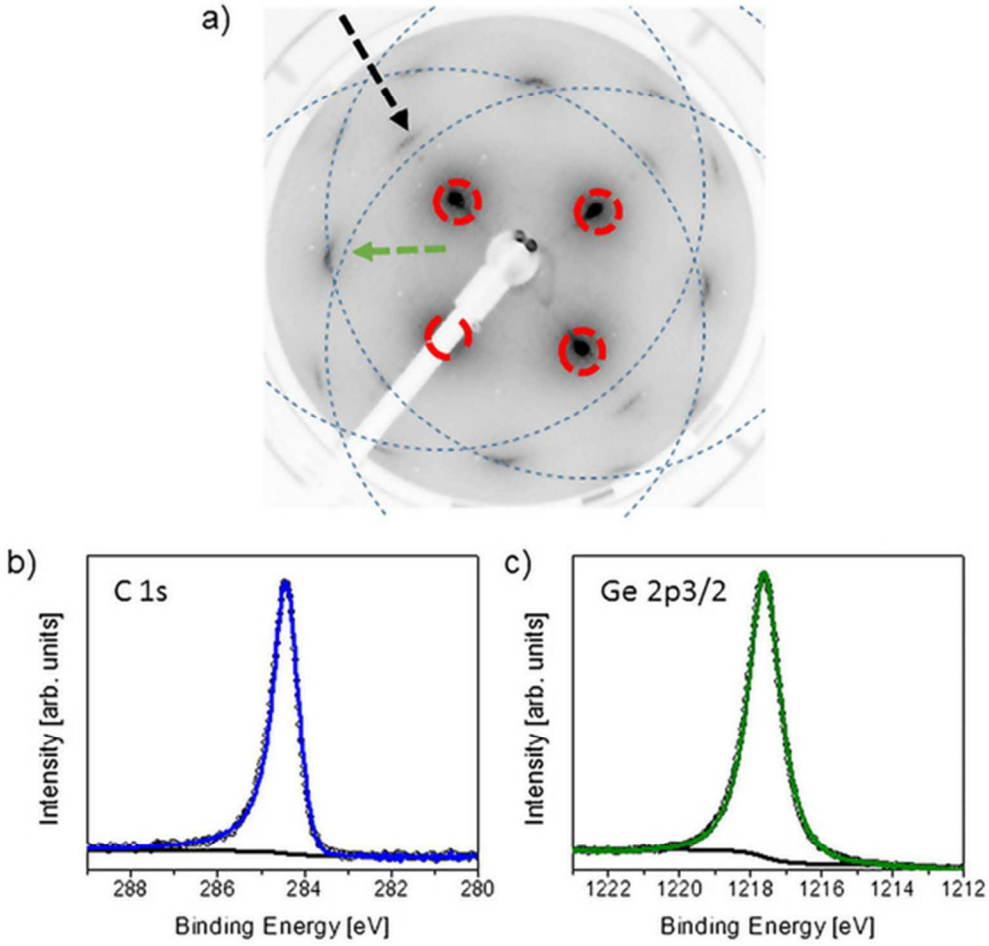

Fig. 4 Low-energy electron diffraction (LEED) and X–ray photoelectron spectroscopy measurements for graphene on the Ge(001)/Si(001) surface. a) LEED spots collected at 56 eV from high-quality Ge(001) are marked with a red circle. LEED shows graphene domains marked with a blue circle. Those domains have two preferred orientations in relation to the Ge(001) surface, marked by a green arrow and a black arrow respectively. b) XPS C 1s XPS spectra taken from graphene Ge(001)/Si(001) indicate the presence of high-quality graphene. c) Ge 2p XPS spectra taken from Ge.
48x46mm (300 x 300 DPI)

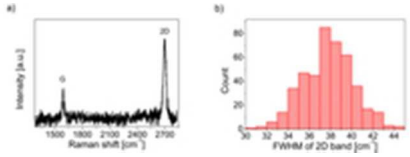

Fig 5. a) Raman spectrum of graphene on Ge(001), b) Histogram of the FWHM of the 2D peak.
17x6mm (300 x 300 DPI)

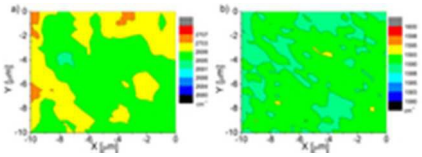

Fig. 6. Micro-Raman maps of a) position of 2D band and b) position of G band.
17x6mm (300 x 300 DPI)

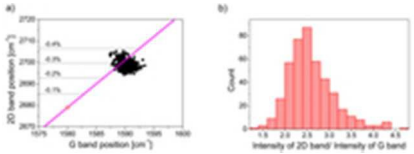

Fig. 7 a) Plot of the position of the 2D band in relation to the position of the G band. The magenta-colored solid line with a slope 2.2 represents the effect of strain on the graphene lattice. b) Histogram of the ratio of intensity of the 2D to the G peaks.
17x6mm (300 x 300 DPI)